Published in final edited form as:
Bioorg Med Chem. 2008 February 15; 16(4): 2114–2130. doi:10.1016/j.bmc.2007.10.081.

Influence of sulfur oxidation state and steric bulk upon trifluoromethyl ketone (TFK) binding kinetics to carboxylesterases and fatty acid amide hydrolase (FAAH)

Craig E. Wheelock[a,b], **Kosuke Nishi**[a], **Andy Ying**[a], **Paul D. Jones**[a], **Michael E. Colvin**[c], **Marilyn M. Olmstead**[d], and **Bruce D. Hammock**[a,*]

[a] Department of Entomology and Cancer Research Center, University of California, Davis, CA 95616

[b] Division of Physiological Chemistry II, Department of Medical Biochemistry and Biophysics, Karolinska Institutet, Scheeles väg 2 SE-171 77 Stockholm, Sweden

[c] School of Natural Sciences, University of California, Merced, CA 95344

[d] Department of Chemistry, University of California, Davis, CA 95616

Abstract

Carboxylesterases metabolize numerous exogenous and endogenous ester-containing compounds including the chemotherapeutic agent CPT-11, anti-influenza viral agent oseltamivir and many agrochemicals. Trifluoromethyl ketone (TFK)-containing compounds with a sulfur atom beta to the ketone moiety are some of the most potent carboxylesterase and amidase inhibitors identified to date. This study examined the effects of alkyl chain length (i.e., steric effects) and sulfur oxidation state upon TFK inhibitor potency (IC_{50}) and binding kinetics (k_i). The selective carboxylesterase inhibitor benzil was used as a non-TFK containing control. These effects were examined using two commercial esterases (porcine and rabbit liver esterase) and two human recombinant esterases (hCE-1 and hCE-2) as well as human recombinant fatty acid amide hydrolase (FAAH). In addition, the inhibition mechanism was examined using a combination of ^{1}H NMR, X-ray crystallography and ab initio calculations. Overall, the data show that while sulfur oxidation state profoundly affects both inhibitor potency and binding kinetics, the steric effects dominate and override the contributions of sulfur oxidation. In addition, the data suggest that inclusion of a sulfur atom beta to the ketone contributes an increase (~5-fold) in inhibitor potency due to effects upon ketone hydration and/or intramolecular hydrogen bond formation. These results provide further information on the nature of the TFK binding interaction and will be useful in increasing our understanding of this basic biochemical process.

Keywords

carboxylesterase; esterase; fatty acid amid hydrolase; FAAH; trifluoromethyl ketone; TFK; inhibitor; kinetics; sulfur; benzil; ab initio calculations; intramolecular hydrogen bond

*Corresponding Author: Dr. Bruce D. Hammock, Department of Entomology, University of California, Davis, CA 95616, Tel (530) 752-8465, Fax (530) 752-1537, email: E-mail: bdhammock@ucdavis.edu.

Supplementary data
Supplementary Figure S1 provides a version of Figure 7 that includes FAAH in the alignment.

1. Introduction

Carboxylesterases (CaEs) are members of the α/β hydrolase-fold family of enzymes that play a role in a broad range of biological processes.[1–3] They are responsible for the hydrolysis of numerous exogenous and endogenous ester-containing compounds[4, 5] and have become of increased interest due to their utility in the activation of prodrugs and metabolism of softdrugs,[6] including the chemotherapeutic agent CPT-11[7] and the anti-influenza viral agent oseltamivir[8]. CaEs are also important in agrochemical research because they detoxify pyrethroid, organophosphate and carbamate insecticides.[9, 10]

Some of the most potent CaE inhibitors identified to date include the trifluoromethyl ketones (TFKs).[11] This moiety was first reported by Brodbeck et al. for use in the inhibition of acetylcholinesterase with potential application as anti-personnel agents.[12] This moiety has since been successfully used to inhibit a range of other enzymes including proteases,[13] phospholipases,[14] fatty acid amide hydrolase (FAAH)[15] as well as CaEs[11, 16, 17] (see Abeles and Alston[18] for a review of enzyme inhibition by fluorine-containing compounds). These enzymes all share a common inhibition mechanism via nucleophilic attack at the electron deficient carbonyl carbon atom in the TFK moiety. The fluorine atom has been extensively employed as a substituent in the synthesis of enzyme inhibitors due to its steric compactness, electronegativity and exogenous nature (few endogenous compounds contain fluorine).[18] It is particularly useful for the preparation of inhibitors that are based upon substrate analogs because fluorine is the smallest substituent available for the replacement of hydrogen.[19] The steric effects of fluorine substitution are therefore minimal, but fluorine is strongly electron attracting and inductive effects are often prominent features of fluorine-containing compounds. TFK-containing compounds (and polyfluoroketone compounds in general) can form tetrahedral enzyme:inhibitor complexes that possess structural resemblance to transition state species. Subsequently, binding forces that ordinarily stabilize the transition state species can thus stabilize the hemiketal adduct so that the rates and equilibria for dissociation are remarkably low in many cases.[20] These effects can be achieved with analogs containing fluorine substituents present on either side of the carbonyl (α or α′, see Figure 1), which are also effective esterase inhibitors [21].

Although fluorine substituents can greatly improve the affinity of serine hydrolases for ketones, the inhibitors must also contain other substituents capable of interacting with the specificity-conferring subsites within the active site of the enzyme. For example, a simple structure such as 1,1,1-trifluoropropan-2-one or hexafluroacetone, while containing a TFK moiety, will generally be an ineffective enzyme inhibitor.[22] Consequently, the incorporation of the TFK moiety into inhibitors that exhibit structural similarity to endogenous substrates has proven to be a useful strategy for preparing potent inhibitors of a range of enzymes.[18] This strategy has been employed to generate inhibitors of acetylcholinesterase[12], juvenile hormone esterase[11] and fatty acid amide hydrolase[15]. A number of structure activity relationship studies have further examined the issue and for effective CaE inhibition, the moiety attached to the TFK tends to consist of long alkyl chains (generally 10–12 carbons alpha to the ketone).[11, 23–27] A key structural component in inhibition potency is the inclusion of a sulfur atom beta to the ketone (Figure 1).[28] This atom was initially incorporated into TFK inhibitors to serve as a bioisostere of the olefin in juvenile hormone, the natural substrate of juvenile hormone esterase (JHE).[11, 28] It was hypothesized that the electronic environment of a sulfur atom would be an appropriate mimic of the double bond in the α, β-unsaturated ester in juvenile hormone.[11, 28] However, the resulting increase in compound potency was greater then expected based upon endogenous substrate mimicry alone. In addition, the observed increase in inhibitor potency was shown to apply to mammalian CaEs as well, indicating that the sulfur atom had a greater role than simply mimicking the olefin in juvenile hormone.[17, 21]

Three main hypotheses have been generated to explain the role of sulfur in enhancing inhibitor potency. The first hypothesis is that the sulfur atom affects the equilibrium between the TFK ketone and its hydrated state (*gem*-diol). Inhibitors exist as a dynamic equilibrium between those two forms and interconvert based upon their physical properties as well as their local environment (see Figure 1 and Figure 2 for a description of the equilibrium process). It is believed that the active form of a TFK inhibitor is the ketone consisting of triganal planar geometry.[20, 26] However, because these are transition state analog inhibitors, the geometry of the actual enzyme:inhibitor complex is tetrahedral. Therefore inhibitors that favor an equilibrium shift to the *gem*-diol versus the ketone should decrease the abundance of the inhibitory species, but should also favor the retention of the enzyme:inhibitor complex following inhibitor binding (Figure 2). In other words, the kinetics of initial inhibitor binding (the bimolecular rate constant, k_i) would be slowed, but the overall equilibrium would be shifted to the bound inhibitor (effectively decreasing K_i or IC_{50}). These effects have indeed been observed; however they did not explain the full extent of the sulfur contributions to inhibitor binding.[29] A second hypothesis is that the hydrated ketone (*gem*-diol) forms an intramolecular hydrogen bond with the sulfur atom, forming a 5-membered ring (or 6-membered ring in the case of the sulfur oxidation products as shown in Figure 1). This ring would hypothetically stabilize the bound inhibitor and shift the equilibrium towards the enzyme:inhibitor complex. However, this effect could also occur with the free inhibitor, leading to a reduction in the ketone concentration and reducing the apparent inhibitor potency. The formation of an intramolecular hydrogen bond would therefore cause a mixture of effects similar to those observed with the equilibrium shift due to ketone hydration. Studies in this area indicate that intramolecular hydrogen bonding does correlate roughly with inhibitor potency,[29, 30] but is insufficient to account for all of the observed effects. The third hypothesis is that the sulfur atom forms a pi-stacking interaction with aromatic residues in the active site of the enzyme.[29, 31] This interaction would stabilize the bound inhibitor, again shifting the equilibrium towards the enzyme:inhibitor complex. However, in this case, no additional effects upon the ketone/*gem*-diol would be observed. Recent work in this area has shown that this effect is important in JHE inhibition,[31] but it has not been examined in other enzyme systems.

The aim of the current study was to provide increased insight into the nature of the interaction between TFK inhibitors and CaEs, with a special focus on the effects of the sulfur atom beta to the ketone. Because the observed effects appear to be enzyme specific, we examined a number of different mammalian serine hydrolases including multiple CaEs and FAAH. The results show that the role of the sulfur atom in inhibitor binding is complex and appears to be a combination of the above hypotheses, as well as other potential unknown effects. These data will be useful for designing other TFK inhibitors and could potentially be applied to other small molecule-enzyme interactions. Taken together the results from this study clearly demonstrate that the sulfur atom as well as its oxidation products greatly affects TFK inhibitor binding kinetics and potency. However, these effects are counterbalanced by the steric effects of increasing inhibitor size.

2. Results

2.1. IC_{50} determination

The IC_{50} for esterase inhibition by aliphatic TFK-containing compounds was measured using a number of different mammalian CaEs. Focus was placed on the effects of structural changes in the aliphatic chain and sulfur oxidation state. The effects of alkyl chain length were only examined for the porcine esterase, with inhibitor potency generally increasing with the length of the alkyl chain (R in Figure 1) and reaching a maximum at 10 carbons (Table 1 and Figure 3A). The effects of changes in sulfur oxidation state upon inhibitor potency for the porcine esterase were very pronounced, with inhibitor potency generally decreasing on the order of

thioether> sulfoxide>sulfone. However, these effects were dependent upon alkyl chain length, with increasing alkyl chain diminishing the effect of sulfur oxidation state. For example, for compounds with a hexyl alkyl chain (**2, 7, 11**), the thioether derivative was ~37- and 63-fold more potent then the sulfoxide- and sulfone-containing derivatives, respectively. However, for the dodecyl-containing compounds (**5, 10, 14**), the thioether derivative was equipotent to the sulfoxide and only ~3-fold more potent then the sulfone derivative. These data demonstrate that while both alkyl chain length (i.e., steric bulk) and sulfur oxidation affect inhibitor potency, long alkyl chain length exerts a dominant effect. However, a long alkyl chain is needed to overcome the increased polarity of the sulfoxide and sulfone. Data for the other mammalian enzymes examined were essentially consistent with the porcine esterase data. However, the differences between sulfur oxidation states (with alkyl chain kept constant at octyl) were not as pronounced as for the porcine data. In particular, for the hCE-1 enzyme, the sulfone compound (18 nM, **12**) was actually more potent then the thioether derivative (24 nM, **3**). Both hCE-2 and the rabbit esterase demonstrated the same relative potency pattern for sulfur oxidation as the porcine esterase (thioether>sulfoxide>sulfone). In all cases, the methylene analog (1,1,1-triflurododecan-2-one, TFDK, **15**) of the thioether compound (1,1,1-trifluro-3-octylthiopropan-2-one, OTFP, **3**) was consistently less potent. Overall, the majority of the compounds examined were relatively potent inhibitors with low nM IC_{50} values, with notable exceptions of the 4–8 carbon alkyl chain sulfoxide and sulfone-containing compounds for porcine esterase.

The effects of the length of the enzyme:inhibitor incubation time were measured at two different time points (5 and 15 min). Time dependent effects were observed, on a structure, compound and enzyme specific basis. The data can be divided into two distinct groups, compounds with alkyl groups of 4 or 6 carbons and those with 8, 10 or 12 carbons (the only exception is compound **8** with the sulfoxide). Shorter chain compounds demonstrated a much larger time-dependent effect than longer chain derivatives. The most extreme example was the sulfoxide-containing compounds, which demonstrated the greatest time dependence with an ~8.5-fold increase in inhibitor potency between 5 and 15 min incubations for 6- and 8-carbon containing compounds. These effects were dramatically reduced with longer alkyl chains, with the dodecyl analog exhibiting only a 1.4-fold change. The methylene analog (TFDK, **15**) of the 8 carbon alkyl chain thioether-containing inhibitor (OTFP, **3**) evidenced some slight time-dependent inhibition effects being ~4.5- and 4-fold less potent at 5 and 15 min, respectively. Together these data demonstrate that 1) TFKs are slow tight-binding inhibitors that require significant enzyme:inhibitor incubation intervals and 2) the observed effects of sulfur oxidation state upon inhibitor potency are time dependent.

The above described effects were less pronounced for FAAH (Table 2). Overall, TFKs were weaker inhibitors of FAAH relative to CaEs, with the most potent FAAH inhibitor exhibiting an IC_{50} of 84 nM (**5**) as opposed to 1.3 nM (**4**) for porcine esterase. For all compounds examined, inhibitor potency increased with alkyl chain length, with no maximum observed (Table 2). The increase in potency exhibited a linear correlation with the length of the alkyl chain (with r^2 values ranging from thioether: 0.82, sulfoxide: 0.89, sulfone: 0.92; Figure 3B); however it is not appropriate to make any significant conclusions with only 3 compounds. No differences in the trend were observed between 5 min and 15 min incubation times. The effect of sulfur oxidation state was similar to the esterase studies in that inhibition order was thioether>sulfoxide>sulfone for octyl- or decyl-containing compounds, but it differed for dodecyl-containing compounds with thioether>sulfone>sulfoxide. The methylene analog (TFDK, **15**) was ~5–6-fold less potent then the corresponding thioether compound (OTFP, **3**) independent of the enzyme/inhibitor incubation time. The observed time-dependent effects were opposite those of the esterases, with IC_{50} values increasing (becoming less potent) with time (Table 2). However, this effect was not very dramatic, ranging from 1.1–2.1-fold difference between 5 and 15 min for all the inhibitors examined.

Inhibition studies with benzil exhibited results substantially different from that of TFK-mediated inhibition. Benzil was a potent inhibitor for all CaEs examined, however the inhibition was not as potent as the TFK-mediated inhibition (Table 3). Benzil did not inhibit FAAH at any concentration examined. The inhibition kinetics showed very little time dependence, with essentially full inhibition occurring within 1 min following incubation of enzyme and inhibitor (data not shown). As opposed to TFK-mediated inhibition, benzil's IC_{50} values slightly increased with extended enzyme:inhibitor incubation times. However, these increases consisted of a maximum 2.2-fold increase for porcine esterase, while the other 3 enzymes behaved similarly with a maximum 1.6-fold increase in IC_{50} (decrease in potency) with extended incubation times.

2.2. Kinetic studies

The bimolecular rate constant (k_i) was measured for all inhibitors examined in this study (Table 4). Results were generally consistent with IC_{50} data. The four different enzymes examined exhibited similar trends, but slightly different individual effects. Generally, the observed differences in k_i as a function of sulfur oxidation were most profound for the porcine esterase. The rabbit and hCE-2 exhibited intermediate effects and hCE-1showed very small differences with only a 1.5-fold difference between the thioether (**3**) and sulfoxide (**8**) compounds. For all four enzymes examined, the thioether-containing compounds showed the fastest binding with relatively higher k_i values. The k_i values for sulfoxide- and sulfone-containing compounds were roughly equal, with sulfone values being slightly lower than sulfoxide on the average. The k_i ratio of thioether:sulfoxide-containing compounds for porcine esterase inhibition ranged from a high of 20 for the hexyl derivatives to ~1.0 for dodecyl derivatives. Similar effects were observed for k_i ratios with thioether:sulfone-containing compounds, which ranged from 44 for the octyl derivative to a low of 1.7 for the decyl derivative. The data for the other three CaEs were generally similar, with the notable exception of hCE-1, which had a lower value for the octyl sulfoxide (6.74×10^6 $M^{-1}min^{-1}$) then the sulfone (2.47×10^7 $M^{-1}min^{-1}$). Of particular importance is the observation that the difference in k_i values between the sulfur oxidation states generally decreased with increasing alkyl chain length as shown in Figure 4. A maximum was observed for the decyl derivatives, with all three sulfur oxidation states exhibiting essentially identical k_i values. The overall magnitude of the k_i values decreased from the decyl to dodecyl derivatives, however the three different oxidation states still had relatively similar k_i values. It therefore appears that the k_i values converge with the decyl moiety.

2.3. NMR studies

^{1}H NMR was used to examine for intramolecular hydrogen bond formation. The integration values for the *gem*-diol peaks were measured at two different concentrations as shown in Table 5. The hydrogen on the hydroxyl moiety which is farthest down field (Peak 1 in Figure 5) has a shift that is not indicative of a lone hydroxyl moiety. As it is farther downfield and relatively sharper than would be expected for a hydroxyl proton, it is most likely electron deficient, implying that it has a shared hydrogen bond. In addition, it does not shift with decreasing concentration, suggesting that the interaction(s) involved are unimolecular, or intramolecular. The other hydroxyl proton (Peak 2 in Figure 5) does exhibit a significant shift when only one parameter (concentration) is altered. This reaction indicates that this proton is experiencing a set of interactions that is the result of multiple molecules. The ^{1}H-NMR spectra provide two important observations: 1) The OH resonances for the butyl compound (Figure 5A) are broader than the other compounds (hexyl, Figure 5B; octyl, Figure 5C; and decyl, Figure 5D), which all have relatively sharp resonances at 6.34 ppm, corresponding to the proton that is internally hydrogen bonded to the sulfoxide. This response suggests that the longer alkyl chain is reducing the rate of OH exchange (increasing the internal hydrogen bonding strength). 2) The Peak 2 OH resonance at approximately 4.5–4.9 ppm tends to be broader and more susceptible to concentration effects than the resonance at 6.34 ppm. These data suggest that some

intermolecular hydrogen bonding occurs. However, other than the general shape of the Peak 2 OH resonance, concentration-dependent effects were not observed indicating that hydrogen bonding is concentration independent. Overall, it does not appear that alkyl chain length is having a significant effect on either inter- or intramolecular hydrogen bonding. Some low magnitude shifts were observed in the ^{1}H-NMR, but it is not clear that these are due to chain length. The results therefore seem to indicate the presence of a concentration dependant intermolecular hydrogen bond and a concentration independent intramolecular hydrogen bond.

2.4. Quantum chemical calculations

Ab initio calculations were performed to estimate the strength of a putative intramolecular hydrogen bond between the *gem*-diol and the sulfur moiety beta to the ketone (or the sulfur oxidation products) as shown in Figure 1. The study was specifically designed to examine for effects of alkyl chain length upon bond strength in relation to the different sulfur oxidation states. Results showed essentially no effect of alkyl chain length upon the strength of hydrogen bond formation for all 3 sulfur oxidation states (Table 6). However, the strength of the bond was highly dependent upon the sulfur oxidation state on the order of sulfoxide>sulfone>thioether. Interestingly, the difference between each oxidation state was similar at ~3 kcal/mole. These results indicate that the contributions of alkyl chain length to inhibitor binding are through hydrophobic or steric effects as opposed to any internal electronic effects.

The energy required to hydrate the ketone (*gem*-diol formation) as shown in Figure 1 was also estimated using ab initio calculations (Table 7). Again, no effect of alkyl chain length was observed upon the hydration energy. However, sulfur oxidation state-dependent effects on the energy to form the hydrate were observed with sulfone>sulfoxide≫thioether. The relative difference between sulfone and sulfoxide of ~0.7 kcal/mole was small compared to ~3.5 kcal/mole for the sulfoxide and thioether. These data suggest that sulfone and sulfoxide-containing compounds hydrate to a greater extent than the thioether derivatives.

2.5. X-ray structure studies

The crystal structures of four different sulfoxide-containing inhibitors (**6, 7, 8, 9**) were solved to examine for hydrogen bond formation (Figure 6). The structures were characterized by linear chain hydrocarbon stacking of rod-shaped molecules with lateral intermolecular hydrogen bonding interactions between *gem*-diols and sulfoxide groups. However, no intramolecular hydrogen bonds were observed in any of the compounds. Melting points for these crystalline solids were very similar ranging from 79–82 °C for **6**, 89–91 °C for **7**, 87–90°C for **8**, and 90–95°C for **9**.

3. Discussion

The inhibition mechanism of TFKs has been examined by a number of research groups and there is a fair amount of consensus in the field regarding how the TFK moiety interacts with the enzyme. The main outstanding issues revolve around the hydration state of the “active” form of the inhibitor and the secondary interactions that occur within the active site of the enzyme that can affect inhibitor binding (mainly van der Waals interactions and electronic interactions such as pi-stacking). The issue of the geometry of the TFK in its active form (i.e., inhibitory form) has not been directly addressed in CaEs, but it has been shown for capthepsin B,[32] acetylcholinesterase[20] and chymotrypsin[33] that the ketone is the inhibitory species. These findings were further supported for CaEs by Roe et al., who postulated that the ketone is the inhibitory species for juvenile hormone esterase (JHE) inhibition,[34] which has been supported by 3-D QSAR studies[26]. Therefore, it is probable that the ketone is also the inhibitory species

in TFK-mediated CaE inhibition, although conflicting results suggesting that the *gem*-diol was the active form of the inhibitor have been published.[30]

The current study was designed to explore some of the remaining questions of the physicochemical properties affecting TFK hydration and examine their correlation with inhibitor potency. It is well-accepted that TFKs form a hydrate in aqueous solutions, with more potent inhibitors tending to exhibit a greater degree of hydration.[11, 29] In addition, work has shown that the extent of hydration correlates with inhibition potency and that the substituents surrounding the TFK moiety contribute to the ketone hydration.[29, 35] However, it is still uncertain to what extent the substituents affect the binding kinetics. Potent TFKs are considered to be slow tight-binding inhibitors, with equilibrium times on the order of hours to days.[27] However, the rate of binding (k_i) was reported to vary with the substituent beta to the ketone.[29] We therefore measured k_i and IC_{50} values for a range of TFKs containing a sulfur atom of varying oxidation state in the beta position (Figure 1). TFK-mediated inhibition of a non-esterase enzyme, the serine hydrolase FAAH, was also examined in order to test for esterase-specific effects. These data combined with a number of studies on the potential effects of intramolecular hydrogen bonding in the hydrated ketone serve to expand our knowledge of the mechanism of TFK-mediated inhibition of CaEs.

3.1. IC_{50} determinations

The observed IC_{50} values in this study were in agreement with previously published work.[27, 29, 36] Generally, a ten carbon (decyl moiety) chain appears to be the global maximum for optimal inhibitor potency with all of the compounds examined in this study. The only exception was the 5 min sulfone decyl derivative (**13**), but the 15 min derivative held the same pattern (Table 1). These data are consistent with earlier work for mammalian esterases, which typically exhibit an inhibition maximum with alkyl chains of 8–10 carbon atoms beyond the thioether.[27, 36] The time-dependent nature of the inhibition process was observed by measuring the IC_{50} at 5 min and 15 min. An important point is that the 15 min values are most likely not in equilibrium either, but because TFK-mediated inhibition of CaEs appears to exhibit asymptotic behavior,[29] these values are probably relatively close to the equilibrium values. However, as demonstrated by Wadkins et al., the TFK binding process can be extremely slow.[27] Rosell et al. also reported that extended incubation times (0 min vs. 10 min) increased the observed potency of TFK inhibitors.[37] Previous work comparing the IC_{50} values of compounds **2** and **7** (thioether and sulfoxide) showed a strong time-dependent effect. A 30 sec enzyme:inhibitor incubation resulted in **7** being >100-fold less potent then **2**, whereas a 3 h incubation resulted in **7** being only 5-fold less potent.[29] Similar results were observed here, with a 5 min incubation resulting in a 37-fold difference as opposed to a 15 min incubation giving an 18-fold difference. These data further demonstrate the point that if true equilibrium is necessary for experimental design, then much greater incubation times may be required. The majority of the TFK literature published to date, with the exception of work by Wadkins et al.,[27] generally used incubation times of 30 min or less. Accordingly, as the length of incubation can affect both the absolute as well as relative inhibitor potency,[27, 29] it is important that studies on TFKs are aware of the assumptions/limitations in assay formats.

An important observation from the IC_{50} data is the comparison between the thioether-containing derivative OTFP (**3**) and its methylene analog TKDK (**15**). These two compounds have been extensively studied in the literature and OTFP in particular has become a “classical” CaE inhibitor.[11, 16, 28, 29, 31, 34, 37, 38] Numerous studies have shown that inclusion of the sulfur beta to the ketone in OTFP confers increased inhibition potency and as discussed within this paper, a number of theories have been put forward to explain these observations. An examination of the 4 different mammalian esterases examined in this study shows that OTFP is from 2.3–7.4-fold more potent then the TFDK analog, with an overall average of ~5-fold

(Table 1). This potency does appear to have some time-dependence, with longer incubations decreasing the fold difference between OTFP and TFDK. This observation further supports the inhibition mechanism proposed in Figure 2. The sulfur atom shifts the hydration equilibrium towards the *gem*-diol, effectively increasing k_H, reducing ketone concentration and apparent inhibition potency. However, increased incubation times allow for ketone formation and subsequent enzyme inhibition, thereby reducing the observed sulfur effects. These data support earlier studies performed on JHE.[31] However, the magnitude of difference is quite small compared to MsJHE, which demonstrated an approximately 15-fold difference in potency between OTFP and TFDK (Table 1). However, another important aspect of the binding process is the interactions of the inhibitor with non-catalytic residues. Wogulis et al. demonstrated via mutation studies that the sulfur atom beta to the ketone exhibited its effect by forming a pi-stacking interaction with a phenylalanine in the active site of JHE.[31] However, even the F259I mutant still evidenced that OTFP was 5-fold more potent then TDFK. These data therefore suggest that the other physicochemical interactions examined in this study such as contributions to ketone hydration and intramolecular hydrogen, as well as other potential interactions, also play a role in inhibitor binding – all leading to an ~5-fold increase in inhibition potency. A comparison of the sequences for the different enzymes examined suggests that the mammalian esterases do not possess the key aromatic residue to form the pi-stacking interactions (Phe262, Figure 7), potentially explaining the observed differences in sulfur contribution to inhibitor potency between MsJHE and the esterases examined in this study. However, these observations need to be followed up with structural studies for confirmation. Accordingly, the effects of the inclusion of a sulfur atom beta to the ketone upon inhibitor potency are multifaceted and complex and ultimately are at least in part enzyme dependent.

Inhibition of FAAH was examined to test for esterase-specific effects. Previous work had shown that TFK-containing compounds were effective inhibitors of FAAH activity.[15] However, work has shown that inhibitors of FAAH can also inhibit CaE activity, highlighting the issue of inhibitor selectivity for serine hydrolases.[39] FAAH is a mammalian integral membrane enzyme that degrades the fatty acid amide family of endogenous signaling lipids.[40] This class of compounds includes the endogenous cannabinoid anandamide,[41] the sleep-inducing oleamide[42] and the anorexigenic compound oleoylethanolamide.[43] FAAH is a potential pharmaceutical target in the treatment of anxiety, depression and other nervous system disorders[44]. An advantage of working with FAAH is that the endogenous substrate is well understood as opposed to CaEs, whose endogenous role is still in question. The inhibition data were consistent in that for all three sulfur oxidation states, the 12 carbon chain derivative (dodecyl) exhibited the greatest potency. The lack of an observed inhibition maximum suggests that even longer chain aliphatic groups would be potent FAAH inhibitors. However, data reported by Boger et al. for similar derivatives suggest that the inhibition maximum is in fact around 10–12 carbons.[15] While the exact same compounds were not tested in both studies, compound **15** (1,1,1-trifluorododecan-2-one, IC_{50}=1.25 μM) in the present study can be compared with 1,1,1-trifluoroundecan-2-one and 1,1,1-trifluorotridecan-2-one from the Boger et al. study, which found these compounds to only be moderately active inhibitors with IC_{50} values of 0.60 and 0.72μM, respectively. Compounds with longer alkyl chains such as 1,1,1-trifluoropentadecan-2-one exhibited decreased inhibition potency (IC_{50}=2.3 μM).[15] The inhibition data reported by Boger et al. were similar to the data reported here (an ~2-fold difference), which can easily be explained by differences in the assay formats. Boger et al. used ^{14}C oleamide as the substrate as opposed to the fluorescent substrate *N*-(6-methoxypyridin-3-yl)octanamide used in this study. In addition, this study used recombinant human enzyme as opposed to homogenized rat liver. Interestingly, the thioether containing derivative (OTFP, **3**) was an ~5-fold more potent inhibitor of FAAH activity then the methylene analog (TFDK, **15**). These data agree very nicely with the esterase data, suggesting that contributions of sulfur to inhibitor binding are similar for different enzymes. FAAH is evolutionarily distinct from the esterases; however it performs a similar hydrolysis reaction

(with amides as the substrate) and is inhibited by similar compounds. Alignment of FAAH with the esterases shows the low homology between the two divergent groups (Figure S1), making direct sequence-based conclusions difficult. However, the data suggest that the sulfur atom is not undergoing direct pi-stacking interactions as with MsJHE. Accordingly, it is likely that the sulfur atom is affecting inhibitor potency by contributions to ketone hydration and/or intramolecular hydrogen bonding.

Data from the FAAH inhibition studies were interesting in that they demonstrated the opposite trend of the CaE data, with IC_{50} values increasing (decreased potency) from the 5 min to the 15 min incubation. The mechanism behind the differences in the time-dependency of the TFK inhibition is unclear. The catalytic mechanisms of the two enzymes differ because FAAH deviates from the normal Ser-His-Glu/Asp catalytic triad of many serine hydrolases.[5] Instead, FAAH uses a Ser-Ser-Lys triad, where the Lys serves as the base to activate the Ser nucleophile.[45] The Lys residue is believed to strongly activate the catalytic Ser, resulting in a constitutively active nucleophile, enabling FAAH to hydrolyze amides and esters with equal efficiency. It is therefore possible that differences in the architecture of the catalytic triad and/or in the composition of the enzyme active site could account for the differences in binding kinetics. In any case, this work has demonstrated that aliphatic TFK-containing compounds are potent inhibitors of both FAAH and CaEs. It is therefore important that attempts to develop inhibitors for these two divergent pharmaceutical targets ensure selectivity. For example, benzil is a selective CaE inhibitor because no FAAH inhibition was observed at either time point (Table 3). Future FAAH-based studies on inhibitor development need to verify that compounds do not affect CaE activity.

Inhibition of CaE activity by benzil generally agreed with previously published values by Wadkins et al.[46]. Interestingly, studies of benzil-mediated CaE inhibition gave similar results to the FAAH TFK studies, in that for all four esterases examined the 15 min incubation resulted in increased IC_{50} values (decreased potency) relative to the 5 min incubation. However, the mechanism is most likely much different. Work by Fleming et al. examined the nature of benzil binding to hCE-1 via crystallography.[47] They postulated that benzil was actually a very poor esterase substrate and that the benzil inhibition mechanism involved repeated cycling within the active site of the enzyme. This cyclic interaction involves nucleophilic attack by the catalytic Ser221 residue (Ser229 in Figure 7) on one of the benzil carbonyl carbons, forming a covalent intermediate that can reverse to generate benzil and the free enzyme. This process could be described by the k_1 and k_{-1} equilibrium shown in Figure 2. Accordingly, it is possible that esterases turn over benzil during the incubation process, which would explain differences in IC_{50} values between 5 and 15 min. The time-dependent inhibition for hCE-1, hCE-2 and the rabbit esterase were fairly minimal and can be explained by inhibitor hydrolysis. However, the porcine esterase exhibited a ~2.5-fold reduction in inhibition potency from a 5 to 15 min incubation. This decrease is fairly large and unexpected if benzil is acting as a very poor substrate. It is therefore possible that porcine esterase turns over benzil with greater efficiency then the other esterases examined in this study. This point is potentially very interesting and should be further pursued. It would be useful to conduct studies where a range of esterase:benzil incubations were performed from 1 min to >24 h similar to work done by Wadkins et al. for TFKs.[27] It would be beneficial to couple these activity assay studies with quantification of the benzoic acid and/or benzaldehyde hydrolysis products in order to confirm inhibitor turnover. Taken together, these types of studies would provide a great deal of information on inhibitor binding processes for CaEs.

3.2. Kinetic studies

These studies focused on examining the electronic and physical effects of TFK inhibitor structure upon enzyme binding kinetics. Earlier work with porcine esterase had demonstrated

that sulfur oxidation state strongly affected k_i, but did not examine the effects of alkyl chain length.29 The reported differences between the thioether (compound **2**) and the sulfoxide (compound **7**) were quite large at 3.2×10^7 $M^{-1}min^{-1}$ and 9.5×10^5 $M^{-1}min^{-1}$ respectively.[29] These data agree relatively well with those reported in this study (1.05×10^7 $M^{-1}min^{-1}$ and 5.2×10^5 $M^{-1}min^{-1}$, respectively; Table 4), clearly demonstrating that sulfur oxidation state affects inhibitor binding kinetics. However, data provided in the current study show that the effects of sulfur oxidation are less important than the steric effects of increased alkyl chain length. Accordingly, inhibitors with long aliphatic chains (decyl and dodecyl) exhibited essentially identical k_i values for all sulfur oxidation states. However, a clear maximum was observed at 10 carbon atoms (decyl), which is consistent with the IC_{50} data (Table 1). These effects could not be directly examined with the other enzymes in this study because k_i values were only measured for the octyl derivatives. However, the thioether (**3**) and sulfoxide (**8**) data for hCE-1, hCE-2 and rabbit esterase are similar to the porcine esterase data. Conversely, the sulfone (**12**) demonstrated a different pattern, with the porcine esterase having a much slower k_i than the other esterases. There was no overall pattern observed in terms of ordering the enzymes on the basis of k_i, however hCE-2 was generally the fastest (except for the sulfone, in which case it was the second fastest).

Taken together, these data provide insight into the TFK binding mechanism shown in Figure 2. As discussed above, the active form of the inhibitor is still in dispute, but is hypothesized to be the ketone. The inhibition process can be postulated to occur based upon the 4 distinct steps shown in Figure 2. Step **A** shows the equilibrium process between ketone and the *gem*-diol. It has been solidly demonstrated that potent TFK inhibitors favor the *gem*-diol state in aqueous solution.[11, 29] It is therefore expected that the k_H value will be high relative to k_D. Work by Roe et al.34 as well as Rosell et al.[37] has measured K_H values and reported that they are greater for potent inhibitors (i.e., greater degree of hydration). Accordingly, it is expected that the *gem*-diol form of the inhibitor predominates at this step. However, either form could potentially diffuse into the enzyme as shown in Figure 2. If the inhibitor is still in the *gem*-diol form as shown in step **B**, which is the hypothesized mechanism, the inhibitor then needs to undergo a dehydration step to the ketone in step **C**. This step is most likely the rate limiting step of the reaction, which would agree with data published by Brady and Abeles for chymotrypsin inhibition.[33] This mechanism would also explain the time-dependence of both the kinetic and IC_{50} data observed in this study as well as others.[27, 29] For inhibitors such as the sulfoxide and sulfone, which demonstrate significantly slower binding kinetics (i.e, k_i values) relative to the thioether, the dehydration reaction is the key step. Inhibitor potency then becomes a question of significant incubation time. If a potent inhibitor is hydrated to the extent that ketone concentrations are vanishingly small, then k_D will become the limiting step to enzyme inhibition. Indeed, some research groups "correct" K_i values based upon the assumption of actual ketone concentrations relative to total inhibitor concentrations (i.e., the sum of *gem*-diol and ketone levels). This type of correction can subsequently result in K_i values in the low femtomolar range [48]. In a sense, it may therefore be possible to have an inhibitor that is "too hydrated" to be effective over a useful time interval (i.e., <24 h). These observations will be of particular relevance if TFK-containing inhibitors are developed for *in vivo* applications.

3.3. Intramolecular hydrogen bonding studies

The IC_{50} and k_i data demonstrated that sulfur oxidation state had a strong effect upon inhibitor potency and binding kinetics. Previous work had shown that ketone hydration explained a significant amount, but not all, of inhibition potency.[29, 31] It was therefore of interest to determine the mechanism behind these effects. One of the predominant theories regarding the binding mechanism of TFK-containing inhibitors centers around the formation of an intramolecular hydrogen bond as shown in Figure 1.[11, 29, 30, 36, 49] In particular, Filizola et

al. conducted an ab initio study on the relative strength of the intramolecular hydrogen bond, reporting that the bond strength inversely correlated with inhibitor potency.[30] This study therefore attempted to further examine this issue using a number of different methods including ^{1}H-NMR, X-ray crystallography and ab initio calculations. The ^{1}H-NMR and crystallography studies focused on the sulfoxide containing compounds because these were predicted to form the strongest intramolecular hydrogen bond due to the dipole formed by the sulfoxide moiety.[29] Because this intramolecular bond was not observed in the X-ray structures of any of the sulfoxide derivatives (see below), its inferred presence by ^{1}H-NMR is very interesting. Alkyl chain length appears to affect the intermolecular bond, but not the intramolecular bond (Figure 5). However, a limitation in drawing conclusions from this experiment is the fact that spectra were collected in $CDCl_3$ as opposed to water (or D_2O), which would be more representative of the biological environment. The conformations and hydrogen bonding behavior will be different in an aqueous environment, which is the most biologically relevant to this project. However, this approach appears promising and future studies should pursue it to elucidate the formation and strength of the putative intra- and intermolecular hydrogen bonds.

The crystal structure analyses of the sulfoxide-containing inhibitors did not show any intramolecular hydrogen bonding, only intermolecular (Figure 6). This observation is interesting, especially considering that two other sulfur-containing TFK crystal structures, 1,1,1-trifluoro-3-(octane-1-sulfonyl)propane-2,2-diol[29] and 1,1,1-trifluoro-5-phenyl-4-thiapentane-2,2-diol,[50] did contain an intramolecular hydrogen bond. In addition, two sulfur-containing heterocyclic compounds gave mixed results with 3-(2-pyridylthio)-1,1,1-trifluoro-2-propanone showing intramolecular hydrogen bonding and 3-(4-pyridylthio)-1,1,1-trifluoro-2-propanone showing only intermolecular.[51] However, the intramolecular hydrogen bond in 3-(2-pyridylthio)-1,1,1-trifluoro-2-propanone was with the nitrogen in the pyridyl ring and not with the sulfur. One possible explanation is that there are potentially multiple crystal morphologies associated with these compounds. Accordingly, both the crystalline and structural data may depend in part on the conditions of crystallization. It is difficult to interpret the biological significance of these hydrogen bonds, especially considering that bond formation within a crystalline lattice may not be reflective of bond formation in an aqueous system or a protein microenvironment.

Ab initio analysis of the strength of the purported intramolecular hydrogen bond confirmed earlier studies that reported the strength of the intramolecular hydrogen bond between the hydrate and the heteroatom beta to the carbonyl inversely correlate with inhibitor potency.[29, 30] The data in Table 6 show a bond energy of sulfoxide>sulfone>thioether as opposed to the porcine IC_{50} data which are on the order of thioether> sulfoxide>sulfone. There is therefore not a direct correlation between calculated intramolecular hydrogen bond strength and IC_{50}. However, a major caveat to this observation is the extreme time-dependent nature of the sulfoxide TFK binding process. The data in Table 1 are for a maximum 15 min incubation process. However, it has been reported that sulfoxide TFKs can require hours to achieve full binding.[29] An examination of the hCE-1 enzyme shows a different effect, agreeing with the data from Table 6. In addition data from Wadkins et al., who compared 5 min and 24 h enzyme/inhibitor incubations showed the same trend for hCE-1 of sulfoxide=sulfone>thioether,[27] thus making it difficult to draw any general conclusions based upon these data. Some of the data suggest that an intramolecular hydrogen bond does form as shown in Figure 1; however, this putative bond is most likely quite weak. It therefore appears that this effect does contribute to inhibitor binding and/or potency, but is relatively minor compared to other physicochemical interactions.

An interesting correlation was observed between the energy to hydrate the ketone in Table 7 and the IC_{50} data in Table 1. An examination of the correlation for compounds showed an

inverse relationship between alkyl chain length and r^2 value, suggesting that compounds with shorter alkyl chains exhibit more sulfur-oxidation state related effects as opposed to longer chain inhibitors that are predominantly steric. These data support the kinetic studies which showed that k_i values for compounds with short alkyl chains (octyl or shorter) varied on a sulfur oxidation state-dependent basis.

Earlier work by Wheelock et al.[29] calculated the energy to form an intramolecular hydrogen bond of a truncated TFK-containing compound (the alkyl group was a methyl moiety). In comparison to the current study, the absolute value of the numbers is quite different (4.1 and 7.8 kcal/mole for the thioether and sulfone derivatives, respectively). However, the relative differences agree fairly well with a ~3.2 kcal/mole difference between thioether and sulfone in the current study as opposed to 3.7 kcal/mole from Wheelock et al.[29]. As the data in Table 6 demonstrate that alkyl chain does not significantly affect the strength of the putative bond, the discrepancies are most likely due to the calculation methods employed. Similar differences were observed with the ketone hydration energy calculations in Table 7, with earlier published work showing a slightly different trend in the data. Those data reported a trend of sulfoxide>thioether>sulfone (−25.06>−19.51>−17.42 kcal/mole, respectively).[29] The major difference between the ab initio calculations performed in these two studies was the choice of basis set. Earlier work used a 6-31G* basis set as opposed to an aug-cc-pVDZ set for the current study. The double-zeta basis set is preferred because it treats each orbital separately when conducting the Hartree-Fock calculation as opposed to the split-valence basis set, which only calculates a double-zeta for the valence orbital (inner-shell electrons are described with a single Slater Orbital). It is therefore expected that the double-zeta calculations will provide a more accurate representation of each orbital. The asterisk (*) notation on the 6-31G* basis set indicates that p-orbital polarization was taken into account for the calculation. As a check of the data, we re-ran the original data set from the Wheelock et al.[29] study under the reported conditions with the 6-31G* basis set and reproduced the same numbers. Accordingly, the discrepancy between the numbers from the two studies arise from two issues - first, the use of the larger basis set, and second slightly different minimum energy configurations were used. The latter issue is a problem with molecules that have a large number of degrees of freedom. A comparison of the current configurations versus those in the Wheelock et al.[29] study confirmed that the current structures are lower energy. It is therefore expected that the current energies are more reliable then those published in earlier work. These observations demonstrate the point that caution should be used when examining the results of these types of ab initio calculations, and it is often most appropriate to compare relative versus absolute values.

4. Summary

Further work on TFKs should attempt to conclusively address the question of the geometry of the “active” form of the inhibitor. Work performed by the group of Abeles on the active form of peptide-based TFK inhibitors would most likely be an appropriate model.[20, 33] In addition, the potential role of the putative intramolecular hydrogen bond needs to be addressed in greater detail. To date, most studies have attempted to infer the presence and/or role of the bond in inhibitor potency via ab initio calculations[29, 30] or crystallography[29, 51]. Unfortunately, neither of these approaches represents an appropriate study of the potential interactions within a biological system and as such, these studies can only provide suggestive conclusions. The ^{1}H NMR studies produced in this work are a promising start, but are still inconclusive. Further work needs to examine a range of TFK inhibitors consisting of structural variation at the beta moiety (oxygen, sulfur, sulfoxide and sulfone) as well as multiple degrees of fluorination. It would also be of interest to move the heteroatom to the gamma position.[23] A study of this magnitude may be able to conclusively address the issue of intramolecular hydrogen bond formation. Enzyme crystallography studies would also be useful. However, the only esterase structure solved to date with a TFK inhibitor did not show evidence of an intramolecular

hydrogen bond.[31] However, these results were for JHE, and no TFK-containing mammalian structures have been solved to date. One could envision a study in which a mammalian esterase was solved co-crystallized with a number of different heteroatom-containing TFK inhibitors. These data would be very useful in addressing the issue of intramolecular hydrogen bond formation, but could still potentially be criticized as not being reflective of the dynamic environment of a non-crystallized enzyme. It is most likely that with increasing NMR capability, a solution-based esterase structure will eventually be produced. This structure could be probed with a series of TFK inhibitors and given the unique possibility of using a fluorine specific probe, conclusive information regarding the potentially hydrogen bonded inhibitor may be obtainable. In conclusion, this study has shown that 1) inclusion of a sulfur atom beta to the carbonyl increases inhibitor potency by ~5-fold, 2) sulfur oxidation state affects inhibitor binding kinetics, but that steric interactions dominate, 3) the effects of sulfur as well as its oxidation products on inhibitor potency occur through a combination of contributions to ketone hydration and intramolecular hydrogen bonding (as well as other potential effects), and 4) secondary interactions, such as those observed with MsJHE, can profoundly affect inhibition potency, but are enzyme specific. It is clear that in the nearly 30 years since the first report of a TFK-mediated inhibitor of acetylcholinesterase, a great deal of information has been collected regarding the mechanism of these compounds. However, there are still many questions that remain to be answered.

5. Experimental

5.1. Chemicals

All commercial chemicals were purchased from either Sigma Chemical (Saint Louis, MI) or Fisher Scientific (Pittsburgh, PA) and used without further purification. Inhibitors were synthesized according to previously published procedures. Alkyl thioethers (compounds **1–5**) and sulfones (compounds **11–14**) were synthesized as reported previously[36] and sulfoxides (compounds **6–10**) were prepared as reported by Wadkins et al.[27]. 1,1,1-Trifluorododecan-2-one (TFDK, compound **15**) was prepared according to Wogulis et al.[31]. All recrystallizations were performed in dichloromethane/hexane vapor diffusion systems. Compound structure and purity were verified using thin-layer chromatography (TLC) on 10 cm F_{254} silica plates (250 μm thickness, EM Science; Gibbstown, NJ) visualized with either phosphomolybdic acid and heating or 2,4-dinitrophenylhydrazine, GC/MS (HP 6890 GC interfaced with an HP 5973 mass spectrometer, Agilent Technologies; Engelwood, CO) and ^{1}H NMR (Mercury 300, Varian; Palo Alto, CA) as well as melting point when appropriate (Thomas-Hoover apparatus, A. H. Thomas Co.; Philadelphia, PA). In all cases, compounds were greater then 97% pure and structural data agreed with previously published values and are therefore not provided here.

Attempts to purify the butyl sulfone derivative were unsuccessful and a number of different synthesis efforts were attempted. The thioether starting material was mixed for 4 days with 3eq of the peracid. Analysis of the crude reaction showed formation of the sulfone product and excess acid/peracid, with minimal side reactions. The reaction mixture was then divided into 2 portions, with one portion stored over KF for 2 h. However, both ^{1}H and ^{13}C NMR of the filtrate showed 100% decomposition of the product. Flash chromatography of the second portion successfully removed all remaining *m*-CPBA, giving the desired product and *m*-CBA acid. However, washing of an aliquot of this mixture with sodium bicarbonate (*sat*) resulted in decomposition and complete loss of product. Attempts at recrystallizing the product were unsuccessful. Subsequently, no enzyme kinetic measurements were performed with the butyl sulfone derivative.

5.2. Preparation of recombinant human carboxylesterases

Recombinant human CaEs hCE-1 and hCE-2 were produced in a baculovirus expression system as shown previously.[52] In brief, High Five cells derived from *Trichoplusia ni* (1×10^6 cells/ml) were inoculated with high titer of the recombinant baculoviruses harboring the hCE-1 or hCE-2 gene. At 72 hours post-infection, the infected cells were harvested by centrifugation (2,000*g*, 20 min, 4°C) and homogenized using a Polytron homogenizer. After ultracentrifugation (100,000*g*, 60 min, 4°C), the supernatant was loaded onto a DEAE anion-exchange chromatography column. The eluted CaE was further purified by preparative isoelectric focusing using a Rotofor apparatus (Bio-Rad Laboratories; Hercules, CA). Protein concentration was determined according to Bradford with bovine serum albumin as the standard.[53]

5.3. Preparation of recombinant human FAAH

Transgenic expression of the human FAAH in baculovirus system was performed using methods previously described.[54] Briefly, the cDNA encoding the human FAAH (GenBank Accession No # NM_001441) was cloned into pAcUW21 and co-transfected into *Spodoptera frugiperda*-derived Sf21 cells with *Bsu*36I-cleaved BacPAK6 viral DNAs (Clontech Laboratories; Mountain view, CA) to produce recombinant baculoviruses harboring the human *FAAH* gene, Ac-hFAAH.[55] *Trichoplusia ni*-derived High Five cells (1×10^6 cells/ml) were inoculated with high titer of Ac-hFAAH. At 72 hours post-infection, the infected cells were harvested by centrifugation at 2,000*g* for 20 min at 4°C and suspended in 50 mM Tris-HCl (pH 8.0) containing 150 mM NaCl, 1 mM EDTA, 1 μM pepstatin, 100 μM leupeptin, and 0.1 mg/ml aprotinin. The cell suspension was then homogenized using a Polytron homogenizer and centrifuged at 10,000*g* for 20 min at 4°C. The microsomal fraction was collected by ultracentrifugation of the supernatant at 100,000*g* for 60 min at 4°C. The pellet was resuspended in 20 mM Tris-HCl (pH 8.0) containing 10% (w/v) glycerol and 1% (w/v) Triton-X 100 and stored at −80°C until use.

5.4. Bimolecular rate constant (k_i) assays

Kinetic analyses of porcine esterase (E.C. 3.1.1.1) were conducted using a porcine liver preparation (Sigma Chemical; Lot no. 102K7062; 184 units/mg protein and 10 mg protein/ml). Working solutions of enzyme were prepared by diluting enzyme in sodium phosphate buffer (pH 7.4, 0.1 M) to obtain an activity of 200–300 mAU/min (~10 μL of esterase solution into 100–150 μL of buffer). The amount of buffer added was varied in order to maintain the enzyme activity in the range of 200–300 mAU/min, therefore the exact concentration of protein added varied from assay to assay, but was constant over a given range of activity.

Inhibitors were dissolved in ethanol to the desired concentration. All assays were conducted in 96-well polystyrene flat bottom microtiter plates (Dynex Technologies, Inc.; Chantilly, VA). Assays were initiated by adding 1 μL of the inhibitor solution to each well and mixing with 140 μL of sodium phosphate buffer (pH 7.4, 0.1 M). Inhibitor concentrations were fixed for all datum points of each compound and never exceeded more than 1% of the total assay volume. Controls were run with solvent blanks and no significant solvent effects were observed. Microtiter plates were incubated until internal temperature reached 37°C, after which 20 μL of enzyme diluted in buffer was added to each well. Plates were then incubated at 37°C for the designated time interval, followed by substrate addition (final concentration 0.5 mM, *p*-nitrophenyl acetate, PNPA). Absorbance was monitored for 2 min at 405 nm using a SpectraMax 340PC384 Microplate Spectrophotometer (Molecular Devices; Sunnyvale, CA).

The natural log of the mean residual activity was recorded for each time interval. Each time point was performed in triplicate. A linear regression function of at least five datum points and a linear coefficient greater than 98% were used for each k_i determination, which was calculated

using the equation $\ln(\upsilon_0/\upsilon) = k_i[I]t$, where $\ln(\upsilon_0/\upsilon)$ is given by the slope, t is time in sec and [I] is the inhibitor concentration.

5.5. IC_{50} determination

Assays were performed as previously described.[36] Briefly, working solutions of porcine esterase (Sigma Chemical; Lot no. 102K7062) were prepared by dissolving 10 μL of esterase in 80 μL of 0.1 M sodium phosphate buffer (pH 7.4, 0.1 M). Inhibitors were dissolved in ethanol to the desired concentration. Assays were run as described above, except 2 μL of inhibitor solution was added to 140 μL of sodium phosphate buffer (pH 7.4, 0.1 M), then serially diluted 2-fold. A total of 20 μL of enzyme diluted in sodium phosphate buffer was added to each standard wells. Control wells received 20 μL of sodium phosphate buffer only. Plates were incubated for 5 or 15 min at 37°C. A linear regression function with at least 98% linear coefficient was obtained by plotting the enzyme residual activity against the log of inhibitor concentration. The linear function consists of at least 5 datum points with a minimum of 2 datum points above and below 50% residual activity. Each datum point consists of three individual analyses.

Determinations of IC_{50}'s for FAAH were performed in 96-well microtiter plates using methods described by Huang et al.[54]. Briefly, 180 μL of 0.1 M sodium phosphate buffer (pH 7.4) containing 1.6 μg of recombinant human FAAH microsomal preparation was added to each well, followed by 1 μL of inhibitor dissolved in ethanol. After 5 min or 15 min of pre-incubation, 20 μL of the fluorescent substrate *N*-(6-methoxypyridin-3-yl)octanamide (final concentration 50 μM) was added to each well and the production of 5-amino-2-methoxypyridine was monitored for 5 min at an excitation wavelength of 302 nm, an emission wavelength of 396 nm, and a cutoff wavelength of 325 nm on a Spectra Max M2 microplate reader. The assay was formatted such that the linear function consisted of at least 5 datum points, with a minimum of 2 datum points above and below 50% residual activity. Each datum point consisted of three individual analyses.

5.6. Intramolecular hydrogen bonding studies

^{1}H NMR experiments were conducted with four TFK-sulfoxides. Each compound was assayed using a Varian Mercury 300 MHz NMR as described above. All samples were prepared in $CDCl_3$ that had been stored over K_2CO_3(s). Each compound was prepared as a 0.038 M and 0.019 M solution (0.50 mL sample volume) and spectra were processed using the MestreC NMR package (http://www.mestrec.com). A polynomial baseline correction was used during the processing of each individual Free Induction decay (FID).

5.7. Ab initio calculations

Ab initio quantum chemical simulations were performed on the hydrated *gem*-diol forms of the sulfoxide, sulfone or thioether compounds with alkyl R-groups with 3, 4, 6, 8 and 10 carbons. Additionally the dehydrated (ketone) forms of the compounds were optimized with alkyl R-groups of 3, 4, and 6 carbons. The alkane chains were built in the fully extended all-trans conformation, consistent with recent experimental data for aqueous-phase saturated alkanes.[56] All structures were optimized using Density Function Theory with the Becke 3-parameter hybrid exchange functional[57] and Lee-Yang-Parr gradient corrected electron correlation functional[58] (B3LYP) using a double zeta correlation consistent basis set with diffuse basis functions (aug-cc-pVDZ) (for overview of basis sets see Cramer[59]). All quantum chemical calculations were performed using Gaussian 03 Rev. C.02. (Gaussian, Inc., Wallingford, CT).[60]

The strength of an intramolecular hydrogen bond between one of the *gem*-diol hydroxyl groups and the sulfoxide, sulfone or thioether sulfur atoms was calculated. These compounds were

reoptimized including internal constraints on the rotations of the *gem*-diol hydroxyl groups to prohibit hydrogen bonding to the sulfur atoms. The intramolecular hydrogen bond energies were then estimated as the difference in electronic energies between the constrained and unconstrained structures. The hydration energies were calculated as the reaction energy to add water to the ketone form of the compounds. In all cases the energies reported are the total electronic energies without enthalpy or free energy corrections.

5.8. X-ray crystal structure determinations

X-ray single crystal diffraction experiments were carried out on a Bruker SMART 1000 with the use of MoKα radiation (λ = 0.71073 Å). Solution and refinement software were SAINT for data reduction, SHELXS97 for solution and SHELXL97 for refinement. Crystallographic data for these structures have been deposited with the Cambridge Crytallographic Data Centre as supplementary publication numbers CCDC 639660 – 639663. Copies of the data can be obtained, free of charge, on application to CCDC, 12 Union Road, Cambridge CB2 1EZ, UK [fax: +44 1223 336033 or e-mail: deposit@ccdc.cam.ac.uk].

$C_7H_{13}F_3O_3S$, **6**, M = 234.23, monoclinic, a = 5.8201(4) Å, b = 22.2114(16) Å, c = 7.8434(6) Å, β = 107.574(2)°, V =1009.66(13) Å^3, space group $P2_1/n$, Z = 4, T = 90(2) K, D_{calcd} = 1.541 Mg m^{-3}, μ(MoKα) = 0.346 mm^{-1}, 11955 reflections measured, 2514 unique (R_{int} = 0.021) used in all calculations. The final *wR*2 was 0.0749 (all data) and R_1(2289 $I > 2\sigma(I)$) = 0.0261. Residual electron density was 0.601 and −0.237 e Å^{-3}.

$C_9H_{17}F_3O_3S$, **7**, M = 262.29, orthorhombic, a = 10.828(3) Å, b = 7.865(2) Å, c = 28.828(8) Å, V = 2455.3(11) Å^3, space group $Pca2_1$, Z = 8, T = 90(2) K, D_{calcd} = 1.419 Mg m^{-3}, μ(MoKα) = 0.293 mm^{-1}, 28516 reflections measured, 7107 unique (R_{int} = 0.048) used in all calculations. The final *wR*2 was 0.1671 (all data) and R_1(6583 $I > 2\sigma(I)$) = 0.0519. Residual electron density was 1.214 and −0.627 e Å^{-3}.

$C_{11}H_{21}F_3O_3S$, **8**, M =290.34, monoclinic, a = 16.776(2) Å, b = 7.8174(11) Å, c = 10.8575(16) Å, β = 93.920(4)°, V = 1420.6(3) Å^3, space group $P2_1/c$, Z = 4, T = 90(2) K, D_{calcd} = 1.358 Mg m^{-3}, μ(MoKα) = 0.260 mm^{-1}, 10608 reflections measured, 3246 unique (R_{int} = 0.054) used in all calculations. The final *wR*2 was 0.1024 (all data) and R_1(3246 $I > 2\sigma(I)$) = 0.0399. Residual electron density was 0.360 and −0.336 e Å^{-3}.

$C_{13}H_{25}F_3O_3S$, **9**, M =318.39, monoclinic, a = 10.840(3) Å, b = 7.781(2) Å, c = 37.836(11) Å, β = 90.271(7)°, V = 3191.5(16) Å^3, space group $P2_1/n$, Z = 8, T = 90(2) K, D_{calcd} = 1.325 Mg m^{-3}, μ(MoKα) = 0.238 mm^{-1}, 33814 reflections measured, 7320 unique (R_{int} = 0.056) used in all calculations. The final *wR*2 was 0.1573 (all data) and R_1(5292 $I > 2\sigma(I)$) = 0.0639. Residual electron density was 0.825 and −1.203 e Å^{-3}.

Supplementary Material

Refer to Web version on PubMed Central for supplementary material.

Acknowledgments

The authors are grateful to two anonymous reviewers who provided valuable critique of the manuscript and to Åsa Wheelock for extensive assistance with figure generation. C.E.W. was supported by an EU Sixth Framework Programme (FP6) Marie Curie International Incoming Fellowship (IIF). P.D.J. was supported by an NIH/NHLBI Ruth L. Kirchstein NRSA Grant (F32 HL078096). This work was supported in part by NIEHS Grant R37 ES02710, NIEHS Superfund Grant P42 ES04699, USDA Grant 35607 17830 and NIEHS Center for Environmental Health Sciences Grant P30 ES05707.

References and notes

1. Ollis DL, et al. Protein Eng 1992;5:197. [PubMed: 1409539]
2. Cygler M, et al. Protein Sci 1993;2:366. [PubMed: 8453375]
3. Heikinheimo P, et al. Structure Fold Des 1999;7:R141. [PubMed: 10404588]
4. Satoh T, et al. Annu Rev Pharmacol Toxicol 1998;38:257. [PubMed: 9597156]
5. Redinbo MR, et al. Drug Discov Today 2005;10:313. [PubMed: 15749280]
6. Bodor N, et al. Med Res Rev 2000;20:58. [PubMed: 10608921]
7. Bencharit S, et al. Nat Struct Biol 2002;9:337. [PubMed: 11967565]
8. Shi D, et al. J Pharmacol Exp Ther 2006;319:1477. [PubMed: 16966469]
9. Sogorb MA, et al. Toxicol Let 2002;128:215. [PubMed: 11869832]
10. Wheelock CE, et al. J Pestic Sci 2005;30:75.
11. Székács, A., et al. Rational Approaches to Structure, Activity, and Ecotoxicology of Agrochemicals. Draber, W.; Fujita, T., editors. CRC Press; Boca Raton, Florida: 1992. p. 219
12. Brodbeck U, et al. Biochim Biophys Acta 1979;567:357. [PubMed: 444532]
13. Brady K, et al. Biochem 1990;29:7600. [PubMed: 2271520]
14. Street IP, et al. Biochem 1993;32:5935. [PubMed: 8018213]
15. Boger DL, et al. Bioorg Med Chem Let 1999;9:265. [PubMed: 10021942]
16. Abdel-Aal YAI, et al. Science 1986;233:1073. [PubMed: 3738525]
17. Ashour MBA, et al. Biochem Pharmacol 1987;36:1869. [PubMed: 3593399]
18. Abeles RH, et al. J Biol Chem 1990;265:16705. [PubMed: 2211585]
19. Pauling, L. The nature of the chemical bond. Ithaca, New York: Cornell University Press; 1960.
20. Allen KN, et al. Biochem 1989;28:8466. [PubMed: 2605196]
21. Quero C, et al. Bioorg Med Chem 2003;11:1047. [PubMed: 12614892]
22. Guthrie JP. Can J Chem 1975;53:898.
23. Linderman RJ, et al. Pestic Biochem Physiol 1987;29:266.
24. Roe RM, et al. J Agric Food Chem 1990;38:1274.
25. Huang TL, et al. Pharmaceu Res 1996;13:1495.
26. Wheelock CE, et al. Bioorg Med Chem 2003;11:5101. [PubMed: 14604674]
27. Wadkins RM, et al. Mol Pharmacol 2007;71:713. [PubMed: 17167034]
28. Hammock BD, et al. Pestic Biochem Phys 1984;22:209.
29. Wheelock CE, et al. J Med Chem 2002;45:5576. [PubMed: 12459025]
30. Filizola M, et al. Quant Struct-Act Relat 1998;17:205.
31. Wogulis M, et al. Biochem 2006;45:4045. [PubMed: 16566578]
32. Smith RA, et al. Biochem 1988;27:6568. [PubMed: 3219354]
33. Brady K, et al. Biochem 1990;29:7608. [PubMed: 2271521]
34. Roe RM, et al. Arch Insect Biochem Physiol 1997;36:165.
35. Linderman, RJ., et al. Reviews in Pesticide Toxicology. Hodgson, E.; Roe, RM.; Motoyama, N., editors. Vol. 1. North Carolina State University; Raleigh: 1991. p. 261
36. Wheelock CE, et al. Chem Res Toxicol 2001;14:1563. [PubMed: 11743738]
37. Rosell G, et al. Biochem Biophys Res Comm 1996;226:287. [PubMed: 8806628]
38. Hammock BD, et al. Pestic Biochem Physiol 1982;17:76.
39. Zhang D, et al. Neuropharmacology. 2007
40. McKinney MK, et al. Annu Rev Biochem 2005;74:411. [PubMed: 15952893]
41. Cravatt BF, et al. Nature 1996;384:83. [PubMed: 8900284]
42. Cravatt BF, et al. Science 1995;268:1506. [PubMed: 7770779]
43. Rodriguez de Fonseca F, et al. Nature 2001;414:209. [PubMed: 11700558]
44. Cravatt BF, et al. Curr Opin Chem Biol 2003;7:469. [PubMed: 12941421]
45. McKinney MK, et al. J Biol Chem 2003;278:37393. [PubMed: 12734197]

46. Wadkins RM, et al. J Med Chem 2005;48:2906. [PubMed: 15828829]
47. Fleming CD, et al. J Mol Biol 2005;352:165. [PubMed: 16081098]
48. Nair HK, et al. J Am Chem Soc 1993;115:9939.
49. Linderman RJ, et al. Pestic Biochem Physiol 1989;35:291.
50. Olmstead MM, et al. Acta Crystallogr 1987;C43:1726.
51. Székács A, et al. Chem Res Toxicol 1990;3:325. [PubMed: 2133080]
52. Nishi K, et al. Arch Biochem Biophys 2006;445:115. [PubMed: 16359636]
53. Bradford MB. Anal Biochem 1976;72:248. [PubMed: 942051]
54. Huang H, et al. Anal Biochem. 2006
55. López-Ferber, M., et al. Baculovirus Expression Protocols. Richardson, CD., editor. Humana Press; Totowa, NJ: 1995. p. 25
56. Tolls J, et al. J Phys Chem A 2002;106:2760.
57. Becke AD. J Chem Phys 1993;98:5648.
58. Lee C, et al. Phys Rev B 1988;37:785.
59. Cramer, CJ. Essentials of Computational Chemistry: Theories and Models. Chichester; John Wiley & Sons: 2004.
60. Frisch, MJ., et al. Gaussian Inc.; Pittsburg, PA: 1998.
61. Thompson JD, et al. Nucleic Acids Res 1994;22:4673. [PubMed: 7984417]
62. Stok JE, et al. Arch Biochem Biophys 2004;430:247. [PubMed: 15369824]
63. Bracey MH, et al. Science 2002;298:1793. [PubMed: 12459591]

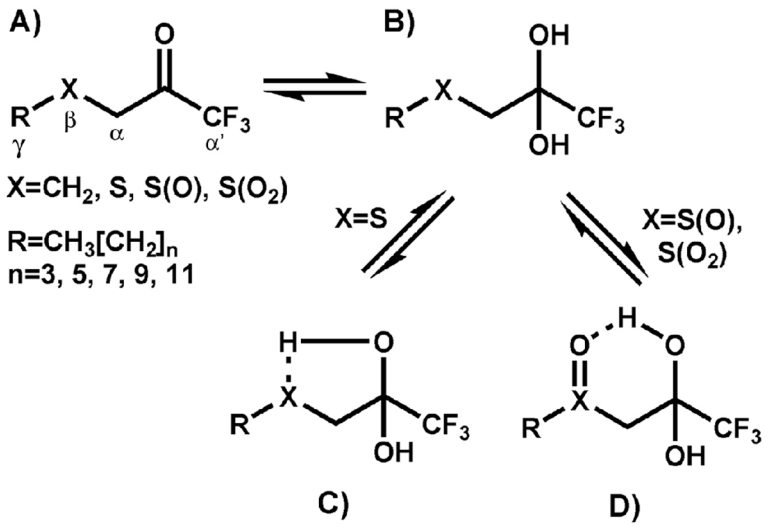

Figure 1.

Structure of inhibitors used in this study. Greek letters refer to atom positioning and are consistent for all compounds. **A)** ketone form of the inhibitor. **B)** *gem*-diol or hydrated form of the inhibitor. **C)** Putative intramolecular hydrogen bond between the *gem*-diol and sulfur atom β to the ketone/*gem*-diol. **D)** Putative intramolecular hydrogen bond between the *gem*-diol and the sulfoxide moiety β to the ketone/*gem*-diol (the sulfone analog is hypothesized to form a similar 6-membered ring upon formation of the putative hydrogen bond).

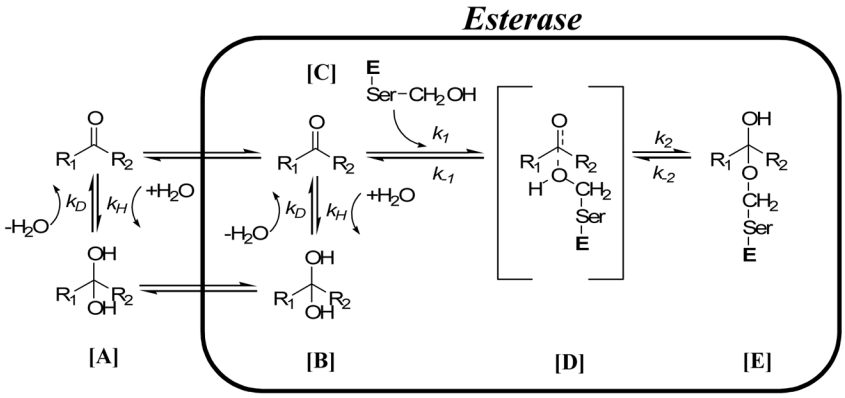

Figure 2.

Potential inhibition pathway for esterases. In **[A]**, the TFK inhibitor establishes an equilibrium between the ketone and *gem*-diol forms. This equilibrium is affected by the R_1 and R_2 moieties and can be described by the rate constants for hydration (k_H) and dehydration (k_D). The equilibrium tends to be shifted towards the ketone for potent inhibitors (i.e, k_D is greater). The ketone or *gem*-diol, or potentially both, then diffuse into the enzyme. It is hypothesized that the ketone is the active form of the inhibitor. Accordingly, if the *gem*-diol form of the inhibitor diffuses into the active site, it needs to undergo a dehydration step from **[B]** to form the ketone in **[C]**. This dehydration step can again be described by the rate constants for hydration (k_H) and dehydration (k_D). The ketone then undergoes nucleophilic attack by the catalytic serine residue forming the transient intermediate in **[D]** according to the rate constant k_1. This intermediate can either collapse as described by k_{-1}, releasing the ketone, or form the hemiketal enzyme/inhibitor complex in **[E]** according to the rate constant k_2. The "Ser" indicates the catalytic serine residue and "E" is esterase.

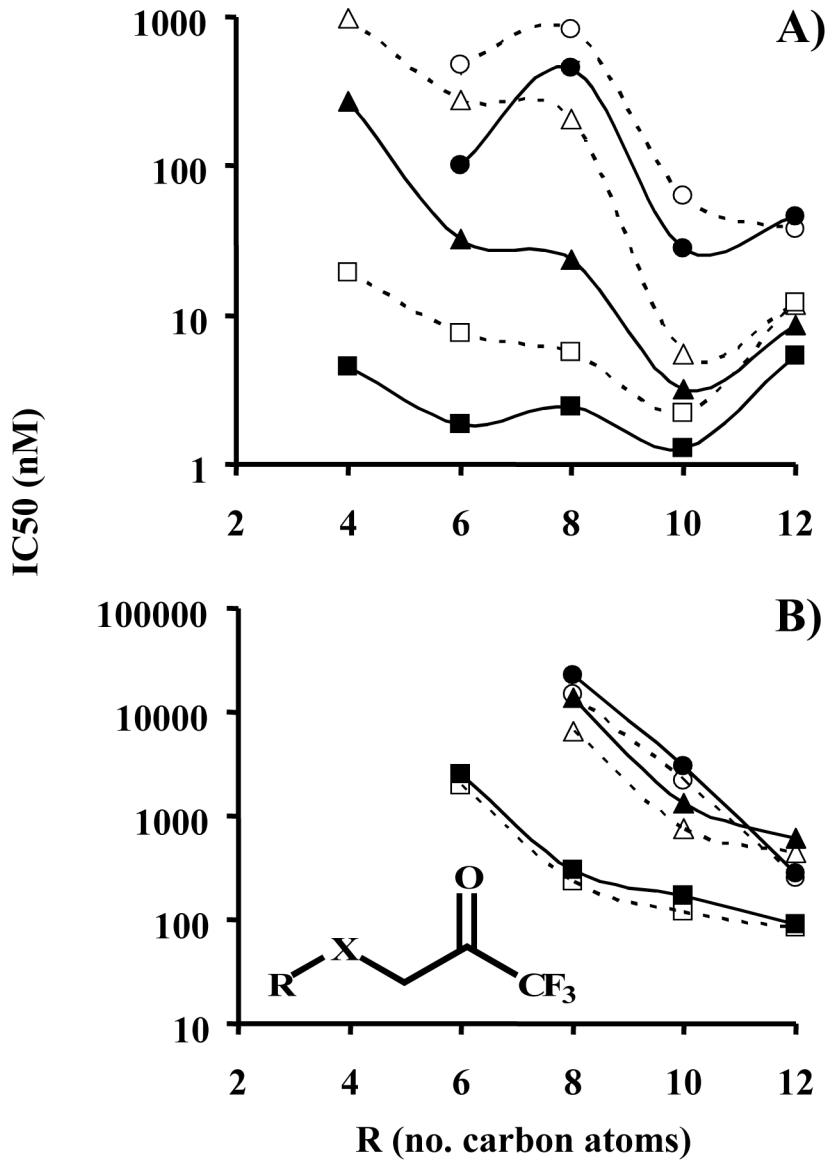

Figure 3.

Effect of alkyl chain length and sulfur oxidation state upon inhibitor potency for A) porcine esterase and B) fatty acid amide hydrolase, FAAH. IC_{50} values were measured following either 5 or 15 min incubation of enzyme and inhibitor. Results are shown as the average ± standard deviation of 3 replicates (error bars are not viewable due to the logarithmic scale, average RSD = 5.4% for esterase and 8% for FAAH). Linear regression values (r^2) for the FAAH curves for R = 6, 8, 10 and 12 carbons were: 5 min 0.94, 0.64, 0.46 and 0.41, respectively; 15 min 0.72, 0.45, 0.47 and 0.48, respectively. If an exponential fit was used, the 15 min values were: 0.99, 0.82, 0.69 and 0.62, respectively. The general inhibitor scaffolding is shown in the insert of graph B, with X being thioether, sulfoxide or sulfone as shown in Figure 1. The graph symbols are: Sulfone 5 min, Sulfone 15 min, Sulfoxide 5 min, Sulfoxide 15 min, Thioether 5 min, Thioether 15 min

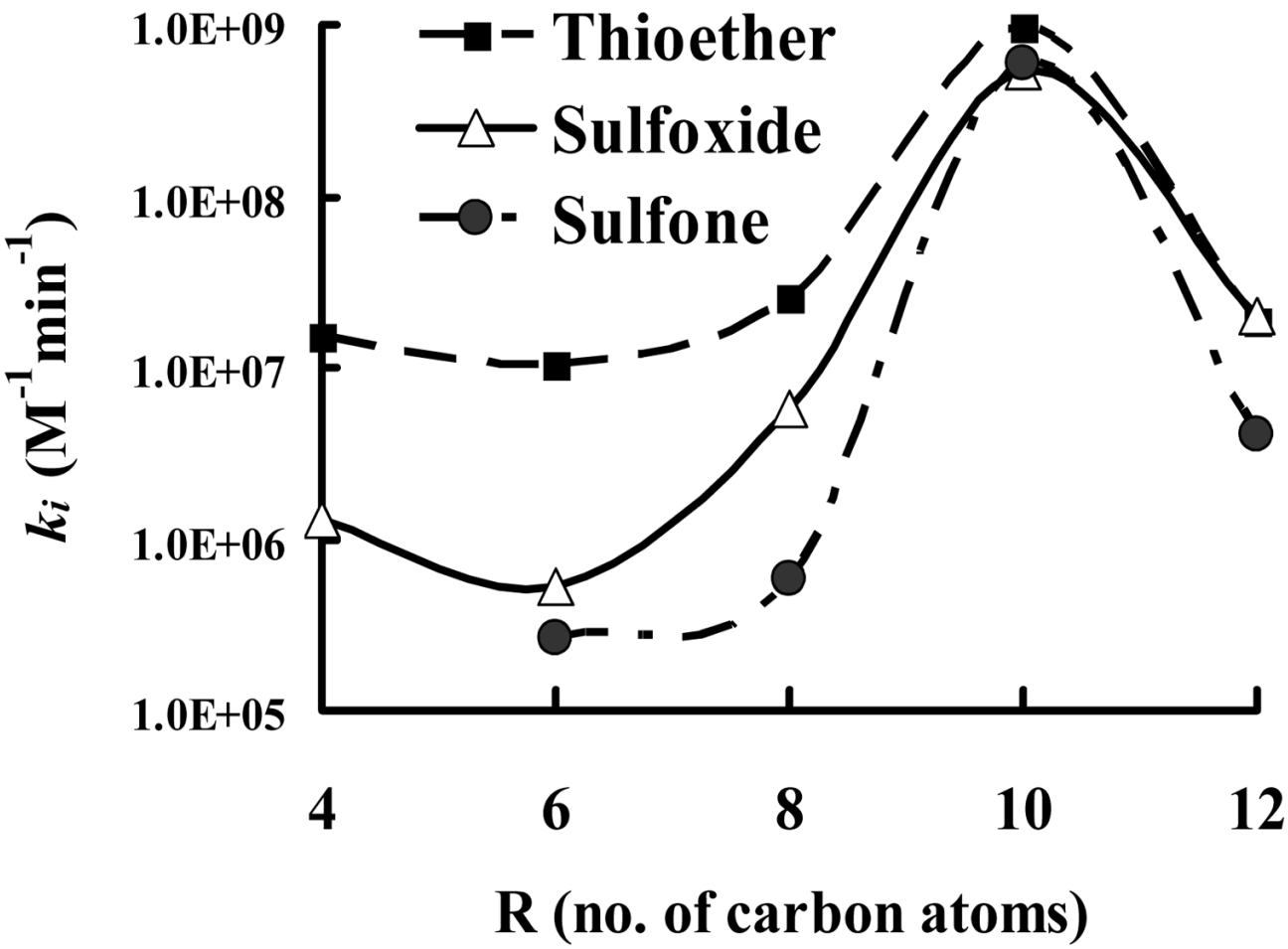

Figure 4.

Effect of carbon chain length upon the bimolecular rate constant k_i. Results are shown as the average ± standard deviation of 3 replicates (error bars are not viewable due to scaling, average RSD ≤ 10%). The general inhibitor scaffolding is shown in the insert, with X being thioether, sulfoxide or sulfone as described in Figure 1.

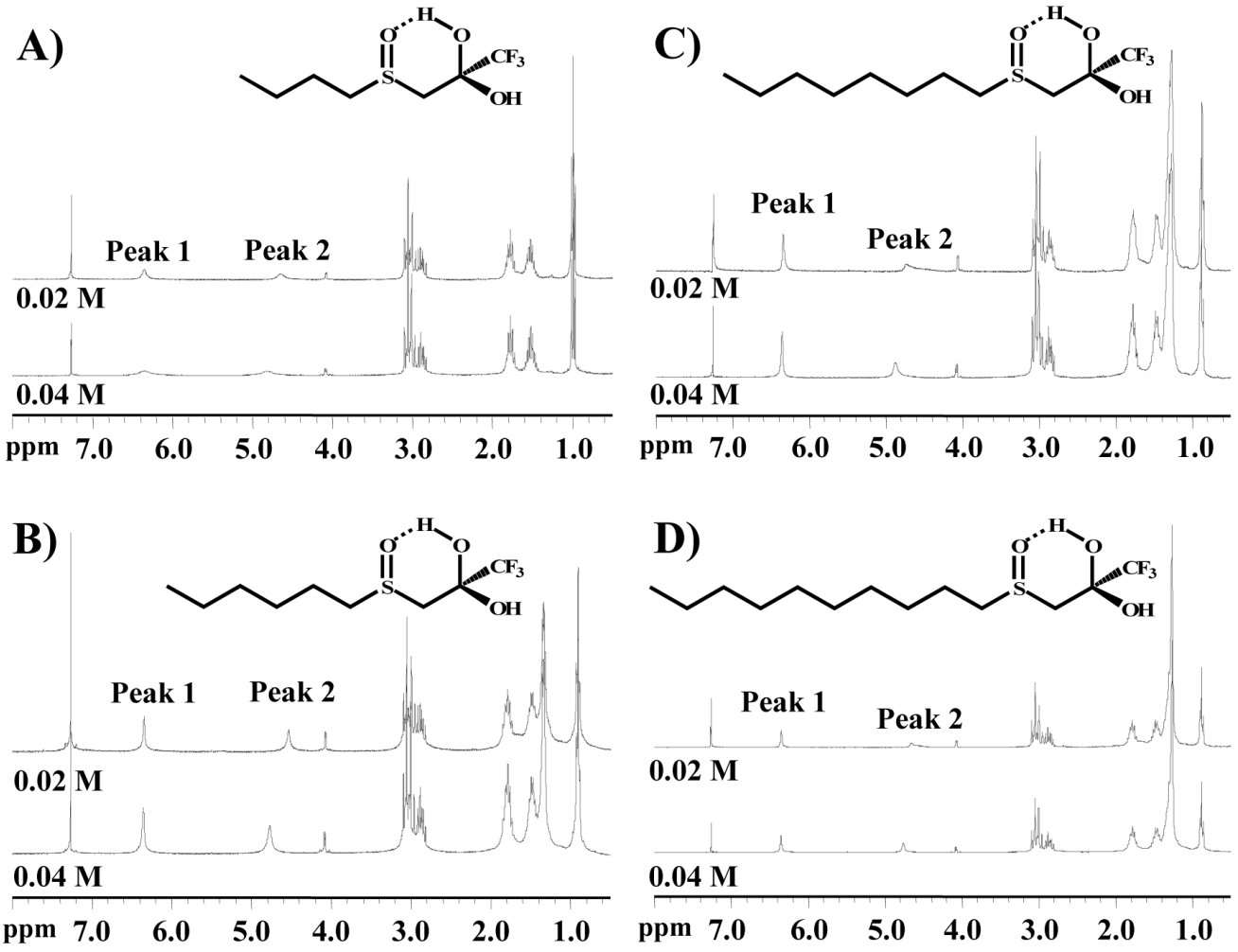

Figure 5.

Effect of alkyl chain length upon hydrogen bond formation for sulfoxide-containing TFK inhibitors. ^{1}H NMR spectra were acquired at two different concentrations of inhibitor (0.02 and 0.04M) in $CDCl_3$. The signals from the *gem*-diol hydroxyls were identified as Peaks 1 and 2. Peak 1 is hypothesized to be the intramolecular hydrogen bonded moiety. Peak integration data are provided in Table 5

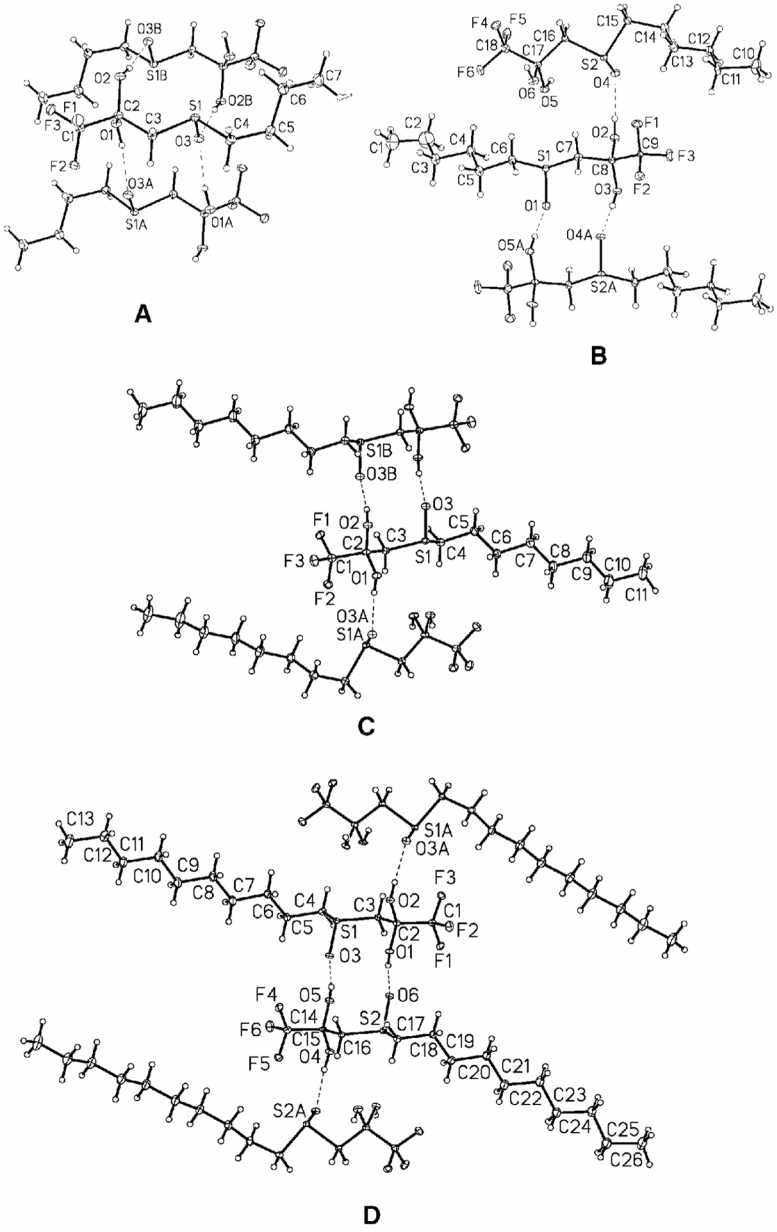

Figure 6.

X-ray crystallographic analysis of sulfoxide derivatives: **A)** 1,1,1-trifluoro-3-(butane-1-sulfinyl)propane-2,2-diol, compound **6; B)** 1,1,1-trifluoro-3-(hexane-1-sulfinyl)propane-2,2-diol, compound **7; C)** 1,1,1-trifluoro-3-(octane-1-sulfinyl)propane-2,2-diol, compound **8; D)** 1,1,1-trifluoro-3-(decane-1-sulfinyl)propane-2,2-diol, compound **9**. Intermolecular hydrogen bonds are shown as dashed lines. No intramolecular hydrogen bonds were observed.

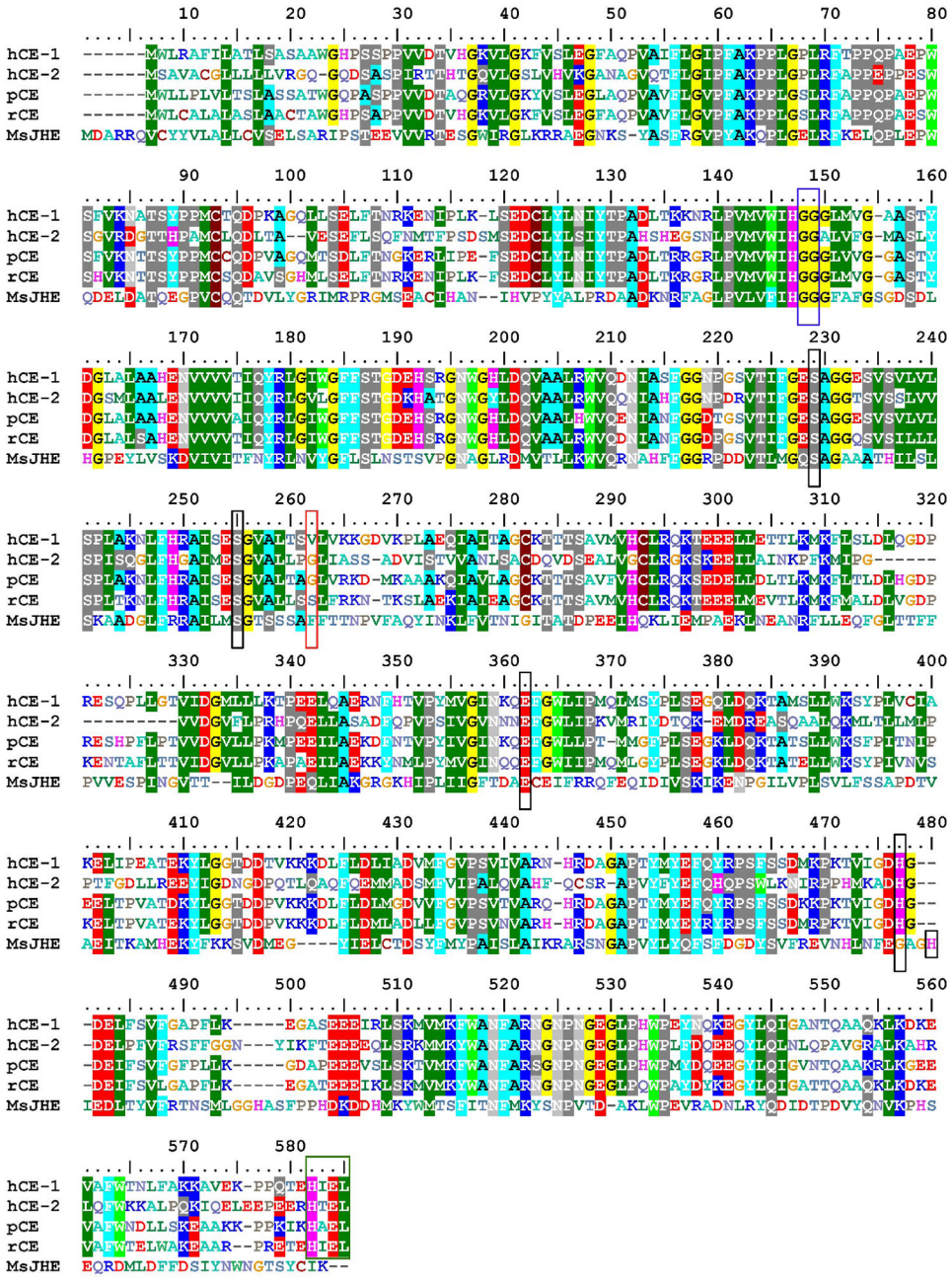

Figure 7.

Alignment of esterases examined in this study using BioEdit v. 7.0.9 (ClustalW alignment[61] using a BLOSUM62 matrix displayed with an 80% threshold). hCE-1=human carboxylesterase 1 (NM_001025194), hCE-2=human carboxylesterase 2 (NM_003869), pCE=porcine esterase (NM_214246), rCE=rabbit esterase (AF036930), MsJHE= juvenile hormone esterase from *Manduca sextra* (AF327882). The catalytic triad is marked with a black box (Ser229, Glu364 and His481; His484 for MsJHE) and the glycines involved in oxyanion hole formation are shown in a blue box (Gly 148 and Gly 149). The putative conserved second serine involved in the catalytic mechanism is also shown in a black box (Ser255).[62] The residue involved in pi-

stacking interactions in MsJHE is marked with a red box (Phe262) and the ER retention sequence is shown in a green box (HXEL).

Table 1

Dependence of esterase IC_{50} upon sulfur oxidation state[a]

	Thioether			Sulfoxide			Sulfone			TFDK[d]		
R[b]	**N°[c]**	**5 min**	**15 min**	**N°**	**5 min**	**15 min**	**N°**	**5 min**	**15 min**	**N°**	**5 min**	**15 min**
					Porcine Esterase							
4	**1**	20±1.4	4.5±0.2	**6**	970±70	270±9		N.D.[e]	N.D.		N.D.	N.D.
6	**2**	7.5±0.3	1.8±0.1	**7**	280±19	33±0.2	**11**	470±59	100±10		N.D.	N.D.
8	**3**	5.6±0.2	2.4±0.1	**8**	200±5	23±2	**12**	830±48	460±44	**15**	25±2	9.3±0.7
10	**4**	2.2±0.1	1.3±0.1	**9**	5.5±0.3	3.2±0.2	**13**	63±8	28±0.4		N.D.	N.D.
12	**5**	12±0.8	5.3±0.2	**10**	12±0.2	8.6±0.2	**14**	37±0.7	46±0.7		N.D.	N.D.
					hCE1							
8	**3**	24±2	13±1	**8**	30±1	5.5±0.5	**12**	18±1	5.4±0.8	**15**	65±5	30±2
					hCE2							
8	**3**	8.5±0.2	5.8±0.5	**8**	11±1	7.4±0.2	**12**	26±1	21±2	**15**	36±4	20±1
					Rabbit Esterase							
8	**3**	6.7±0.2	1.9±0.1	**8**	16±1	5.0±0.1	**12**	55±1	35±1	**15**	42±1	14±1
					MsJHE wild type[f]							
8	**3**	22±3			N.D.			N.D.		**15**	530±32	
					MsJHE F259I mutant[g]							
8	**3**	330±57			N.D.			N.D.		**15**	1,600±150	

	Thioether			Sulfoxide			Sulfone			TFDK[d]		
R[b]	N°[c]	5 min	15 min	N°	5 min	15 min	N°	5 min	15 min	N°	5 min	15 min

[a] All values are given as the average ± the standard deviation of 3 replicates in units of nM. Incubation of enzyme and inhibitor was performed for either 5 min or 15 min before addition of substrate as described in the Experimental.

[b] R refers to the number of carbon atoms in the alkyl chain as shown in Figure 1.

[c] Individual compound numbers.

[d] 1,1,1-trifluorododecan-2-one.

[e] N.D. indicates that value was not determined.

[f] IC_{50} values were measured for *Manduca sexta* juvenile hormone esterase (JHE) using juvenile hormone as the substrate. Inhibitor and enzyme were incubated for 30 min prior to addition of substrate (^{14}C juvenile hormone). Data are from Wogulis et al.[31].

[g] IC_{50} values were measured for a *M. sexta* mutant JHE in which the 259 phenylalanine had been mutated to a isoleucine. Inhibitor and enzyme were incubated for 30 min prior to addition of substrate (^{14}C juvenile hormone). Data are from Wogulis et al.[31].

Table 2

Dependence of FAAH IC_{50} upon sulfur oxidation state[a]

	Thioether			Sulfoxide			Sulfone			TFDK[d]		
R[b]	N°[c]	5 min	15 min	N°	5 min	15 min	N°	5 min	15 min	N°	5 min	15 min
4	**1**	>40,000	>40,000	**6**	>40,000	>40,000		N.D.[e]	N.D.		N.D.	N.D.
6	**2**	1950±250	2500±190	**7**	>40,000	>40,000	**11**	>40,000	>40,000		N.D.	N.D.
8	**3**	230±20	300±30	**8**	6500±650	13,900±900	**12**	14,800±700	22,500±1100	**15**	1250±110	1800±130
10	**4**	120±10	170±20	**9**	760±50	1350±90	**13**	2200±200	3000±230		N.D.	N.D.
12	**5**	84±7.5	89±7.8	**10**	440±50	600±40	**14**	250±10	280±30		N.D.	N.D.

[a] All values are given as the average ± the standard deviation of 3 replicates in units of nM. Incubation of enzyme and inhibitor was performed for either 5 min or 15 min before addition of substrate as described in the Experimental.

[b] R refers to the number of carbon atoms in the alkyl chain as shown in Figure 1.

[c] Individual compound numbers.

[d] 1,1,1-trifluorododecan-2-one.

[e] N.D. indicates that value was not determined.

Table 3

Esterase and FAAH inhibition by benzil[a]

hCE-1		hCE-2		Porcine Esterase		Rabbit Esterase		FAAH	
5 min	**15 min**	**5 min**	**15 min**	**5 min**	**15 min**	**5 min**	**15 min**	**5 min**	**15 min**
27±1.0	43±1.3	38±1.0	44±1.1	370±26	830±34	19±2.0	29±1.7	>40,000	>40,000

[a] All values are given as the average IC_{50} ± the standard deviation of 3 replicates in units of nM. Incubation of enzyme and inhibitor was performed for either 5 min or 15 min before addition of substrate as described in the Experimental.

Table 4

Bimolecular rate constant (k_i) for inhibitor binding to esterases[a]

	Thioether			Sulfoxide			Sulfone			TFDK[b]	
R	**N°[c]**	k_i	**SD**	**N**	k_i	**SD**	**N**	k_i	**SD**	**N**	k_i	**SD**
					Porcine Esterase							
4	**1**	1.53×10^{7}	3.0×10^{5}	**6**	1.30×10^{6}	5.0×10^{4}		N.D.[d]	N.D.		N.D.[c]	N.D.
6	**2**	1.05×10^{7}	7.5×10^{5}	**7**	5.20×10^{5}	3.5×10^{4}	**11**	2.67×10^{5}	2.4×10^{4}		N.D.	N.D.
8	**3**	2.53×10^{7}	1.6×10^{6}	**8**	5.72×10^{6}	3.2×10^{5}	**12**	5.76×10^{5}	3.5×10^{4}	**15**	2.07×10^{7}	1.2×10^{6}
10	**4**	9.80×10^{8}	1.4×10^{7}	**9**	5.44×10^{8}	1.8×10^{7}	**13**	5.88×10^{8}	5.6×10^{7}		N.D.	N.D.
12	**5**	1.86×10^{7}	3.8×10^{5}	**10**	1.97×10^{7}	1.2×10^{6}	**14**	4.10×10^{6}	1.3×10^{5}		N.D.	N.D.
					hCE1							
8	**3**	1.02×10^{7}	6.2×10^{5}	**8**	6.74×10^{6}	1.7×10^{5}	**12**	2.47×10^{7}	7.5×10^{5}	**15**	6.67×10^{6}	2.0×10^{5}
					hCE2							
8	**3**	3.48×10^{7}	1.9×10^{6}	**8**	1.08×10^{7}	7.8×10^{5}	**12**	4.27×10^{6}	1.4×10^{5}	**15**	2.29×10^{7}	1.2×10^{6}
					Rabbit Esterase							
8	**3**	1.71×10^{7}	6.1×10^{5}	**8**	5.12×10^{6}	1.7×10^{5}	**12**	4.04×10^{6}	1.2×10^{5}	**15**	4.39×10^{6}	2.2×10^{5}

[a] All values are given as the average ± the standard deviation of 3 replicates in units of $M^{-1}min^{-1}$.

[b] 1,1,1-trifluorododecan-2-one

[c] Individual compound numbers.

[d] N.D. indicates that value was not measured.

Table 5

Concentration effects on hydroxyl peak shifts in sulfoxide derivatives[a]

		Chemical Shift (ppm)				Integrated Area			
		0.02M		0.04M		0.02M		0.04M	
R[c]	N°[d]	Peak 1[e]	Peak 2	Peak 1	Peak 2	Peak 1	Peak 2	Peak 1	Peak 2
4	**6**	6.34	4.62	6.31	4.80	0.56	0.49	0.52	0.51
6	**7**	6.33	4.53	6.34	4.77	0.75	0.73	0.70	0.94
8	**8**	6.34	4.66	6.34	4.88	0.72	0.62	0.76	0.50
10	**9**	6.34	4.58	6.35	4.73	0.58	0.50	0.61	0.57

[a] ^{1}H NMR experiments were conducted with four TFK-sulfoxides using a Varian Mercury 300 MHz NMR. All samples were prepared in $CDCl_3$ that had been stored over K_2CO_3(s). Each compound was measured at 0.019 M and 0.038 M.

[b] Relative area units as determined from the ^{1}H NMR analysis.

[c] R refers to the length of the alkyl chain as shown in Figure 1.

[d] Individual compound numbers.

[e] Peak 1 and Peak 2 refer to the hydroxyl groups from the *gem*-diol as shown in Figure 5.

Table 6

Energy to form intramolecular hydrogen bond (kcal/mole)[a]

R[b]	Sulfur oxidation state		
	Thioether	Sulfoxide	Sulfone
3	7.18	13.59	10.39
4	7.25	13.62	10.45
6	7.22	13.64	10.42
8	7.25	13.75	10.45
10	7.28	13.74	10.47

[a] Values were calculated as the amount of energy required to break the intramolecular bond in the 5-membered ring for thioether-containing compounds or the 6-membered ring for sulfoxide- and sulfone-containing compounds as shown in Figure 1.

[b] R refers to the length of the alkyl chain as shown in Figure 1.

Table 7

Energy to hydrate ketone (ΔE kcal/mole)[a]

R[b]	Sulfur oxidation state		
	Thioether	Sulfoxide	Sulfone
3	−12.29	−15.74	−16.51
4	−12.23	−15.67	−16.44
6	−12.24	−15.67	−16.42

[a] Values were calculated for the amount of energy required to hydrate the ketone (form the *gem*-diol) as shown in Figure 1.

[b] R refers to the length of the alkyl chain as shown in Figure 1.